

Hepatic differentiation and transcriptional profile of the mouse liver epithelial progenitor cells (LEPCs) under the induction of sodium butyrate

Wenlin Li¹, Pu You¹, Qing Wei², Yao Li², Xuping Fu², Xiaoyan Ding³, Xin Wang^{3,4}, Yiping Hu¹

¹Department of Cell Biology, Second Military Medical University, Xiangyin Rd. 800, Shanghai 200433, P. R. China, ²State Key Laboratory of Genetic Engineering, Institute of Genetics, School of Life Science, Fudan University, Shanghai 200433, P. R. China, ³Key Laboratory of Stem Cell Biology, Shanghai Institutes for Biological Sciences, Chinese Academy of Sciences, 320 Yue Yang Road Shanghai 200031, P. R. China, ⁴The Stem Cell Institute, Department of Laboratory Medicine and Pathology, University of Minnesota, 2001 6th street SE, Minneapolis, MN 55455

TABLE OF CONTENTS

1. Abstract
2. Introduction
3. Methods and materials
 - 3.1. Establishment of the liver progenitor cell line and treatment with sodium butyrate
 - 3.2. RNA Isolation
 - 3.3. Construction of microarrays and probe preparations
 - 3.4. Microarray hybridization
 - 3.5. Detection and Analysis
 - 3.6. Quantitative Polymerase Chain Reaction
4. Results and Discussion
 - 4.1. LEPCs gave rise to functional hepatocyte after sodium butyrate exposure
 - 4.2. Gene clustering of microarray data
 - 4.3. Sodium butyrate-mediated growth inhibition is associated with the decreased expression of cyclin B1 and Cdk4
 - 4.4. Up-regulated clusters contained mature hepatocyte functional genes which are consistent with the phenotype changes of LEPCs after sodium butyrate treatment
 - 4.5. Down-regulated clusters contained a set of genes may synergistically involved in the stemness maintaining and the process of hepatic differentiation
 - 4.6. The authenticity of microarray data was confirmed by Real-time PCR analysis.
5. Acknowledgement
6. References

1. ABSTRACT

The liver regenerates by progenitor cells when it is damaged in chronic liver diseases and extensive damage. The progenitor cells, also termed “oval cells” according to their morphological traits, can differentiate into hepatocytes and bile duct cells *in vivo*. To better understand the transcriptional pattern that accompanies the hepatic differentiation of oval cells, we applied cDNA microarray to analyze the oval cell-derived liver epithelial progenitor cells (LEPCs) during *in vitro* induced differentiation. Upon exposure to sodium butyrate, a histone deacetylase inhibitor, cultured LEPCs differentiate and express functional hepatocyte markers albumin, tryptophan 2, 3-dioxygenase and alcohol dehydrogenase. For expression profiling, cells were harvested at 6h, 12h, 1d, 3d and 7d after exposure to sodium butyrate. After analyzing the microarray data by SOM clustering, total of 796 differentially regulated genes were grouped into 48 clusters. Consistent with the phenotype change of LEPCs

after sodium butyrate treatment, many hepatocyte functional genes are revealed by analyzing the clusters containing genes up-regulated through all the time points. The clusters, containing down-regulated genes immediately after the induction, are also analyzed. The microarray data was validated by analyzing the expression of selected genes by quantitative real-time PCR. A set of genes expressed synergistically in these clusters may play a central role during the process of differentiation. Sodium butyrate decreases cyclin B1 and Cdk4 expression, which would be associated with LEPCs growth arrest shortly after treatment. Bmi1, a polycomb group protein, is also down-regulated immediately after treatment and remains at a low level during the induction. These findings highlight the key molecular mechanisms by which sodium butyrate, mediates its effects on cell growth arrest and induction of differentiation. In conclusion, our data reflect a global view of gene expression during hepatic differentiation of LEPCs induced by sodium butyrate.

2. INTRODUCTION

The existence of the liver stem cells has been widely accepted since the last decade (1). Extensive studies(2-4), investigating liver regeneration under the conditions when the proliferation of mature hepatocytes was substantially suppressed, demonstrate the emergence and proliferation of small, oval-shaped cells in the periportal area contributed to injured liver regeneration. These cells, termed as oval cells according to their morphological traits, express embryonic liver markers as well as those which are common to hepatocytes and cholangiocytes (5). Oval cells were adult liver progenitors with the potential to give rise to both hepatocytes and bile duct cells during liver regeneration (6). However, the molecular mechanisms of oval cell proliferation and differentiation remain elusive.

The *in vitro* cultured liver progenitors were valuable model to explore the molecular events during liver development and liver regeneration after injury. HBC-3, a hepatic stem cell line, maintained in the undifferentiated state can be induced to differentiate along the hepatocyte lineage in response to DMSO (7). cDNA microarray analysis implicates down-regulation of the Wnt/beta-catenin pathway accompanied by the repression of TCF target genes during hepatic specification of HBC-3. Atsushi Suzuki and his colleagues reported when all endogenous C/EBP family members' function was inhibited in clonally cultured hepatic stem cells by dominant-negative protein A-C/EBP, they stopped differentiating to hepatocyte-lineage cells and proliferated actively (8). All this findings, highlighting the molecular events during the hepatic specification of *in vitro* cultured liver progenitors, would be significant to understand the regulation of liver development and regeneration.

When exposed to sodium butyrate (SB) *in vitro*, oval cell line OC/CDE stop proliferating, increase in size, and express a few hepatocyte molecules, including albumin (Alb) and glucose-6-phosphate (9). LEPCs, the putative mouse oval cell lines established in our lab, also acquired hepatic phenotype after exposure to SB. Considering cDNA microarray technology, which allows the simultaneous analysis at gene expression levels for thousands of transcripts (10, 11), we utilized the murine cDNA microarray to investigate the expression pattern of LEPCs during the time course of SB treatment. Based on the expression profile of LEPCs, we identified 48 gene clusters via SOM, and a group of genes differentially expressed in the LEPCs, which may be specific to the process of LEPCs differentiation.

3. MATERIALS AND METHODS

3.1. Establishment of the liver progenitor cell line and induction with sodium butyrate

The establishment of LEPCs was described as reported previously (12). LEPCs 2 (LEPCs clone 2) was used in the following studies. The cells were cultured on 90 mm dishes, when cells grow to 80% confluence, culture media were replaced with new media contained 5 mM SB

(sigma, MO). The cells were harvested at 0h, 6h, 12h, 1d, 3d, 7d after SB induction for gene expression analysis.

3.2. RNA Isolation

Cells were homogenized in TRIzol (Biostar, Shanghai, China). After centrifugation, the supernatant was separated from the organic phase and was extracted in an equal volume of chloroform. The aqueous phase was then precipitated by an equal volume of isopropanol at 4°C, centrifuged to pellet the RNA and dissolved in Milli-Q water.

3.3 Construction of microarrays and probe preparations

The construction of the microarrays used in this study (BioStarM-80S) was carried out following Brown's method (13). The BioStarM-80S microarrays consisted of 8,464 sequences including full-length and partial cDNAs representing known, novel, and control genes provided by United Gene Holdings. All the sequences were verified. The known genes were selected from the NCBI Unigene set and cloned into a plasmid vector. The novel genes were obtained through systematic full-length cloning efforts carried out at United Gene Holding. The control spots of non-mouse origin in the BioStarM-80S chip included positive reference genes (96 spots), negative reference genes (16 spots), and spotting solution alone without DNA (16 spots). The cDNA inserts were amplified by use of the polymerase chain reaction (PCR) using universal primers to plasmid vector sequences and were then purified (14). All PCR products were examined by agarose gel electrophoresis to ensure the quality and the identity of the amplified clones as expected. Then the amplified PCR products were dissolved in a buffer containing 3×SSC solution. The solution with amplified PCR products were spotted onto silylated slides (Home made) using a Cartesian PixSys 7500 motion control robot (Cartesian Technologies, Irvine, CA., USA) fitted with ChipMaker Micro-Spotting Technology (TeleChem International, Sunnyvale, CA., USA). The glass slides were then hydrated for 2 hrs in 70% humidity, dried for 0.5 hrs at room temperature, and UV crosslinked (65 mJ/cm). They were further processed at room temperature by soaking in 0.2% sodium dodecyl sulfate (SDS) for 10 min, distilled H₂O for 10 min, and 0.2% sodium borohydride (NaBH₄) for 10 min. The slides were dried again and ready for use. The fluorescent cDNA probes were prepared through reverse transcription of the isolated mRNAs and then purified according to the methods of Schena et al (10; 11). The RNA samples from LEPCs without exposure were labeled with Cy3-dUTP and those from LEPCs induced by SB were labeled with Cy5-dUTP.

3.4. Microarray hybridization

The probes were dissolved in 20 µl of Hybridization Solution (5×SSC, 0.4% SDS, 50% formamide). Microarrays were pre-hybridized with a hybridization solution containing 0.5 mg/ml denatured salmon sperm DNA at 42°C for 6 hrs. Fluorescent probe mixtures were denatured at 95°C for 5 minutes, and then applied onto the pre-hybridized chips under the cover glasses. Chips were hybridized at 42°C for 15-17 hours.

Table 1. Primers used for Real-time PCR

Gene symbols		Primers	Products size
<i>Akr1b3</i>	Forward	5'-CAAGCCTGAAGATCCGTCTC-3'	232bp
	Reverse	5'-CACCTCCAGTTCTGTGT-3'	
<i>Bmi1</i>	Forward	5'-TGTCAGGTTCAAAAACCA-3'	184bp
	Reverse	5'-TGCAACTTCTCCTCGGTCTT-3'	
<i>Cnbp</i>	Forward	5'-CCTCGTCTCTCCGTGACATC-3'	155bp
	Reverse	5'-GCATTGCTCTCGTCTCTCT-3'	
<i>Fbxw7</i>	Forward	5'-CCATGTTTCAGCAACACCAAC-3'	230bp
	Reverse	5'-TGGAAGTGGGGCTCTATCAC-3'	
<i>Gcl</i>	Forward	5'-AGGCTCTCTGCACCATCACT-3'	203bp
	Reverse	5'-TGGCACATTGATGACAACCT-3'	
<i>Gstm1</i>	Forward	5'-AGAACCAGGTCATGGACACC-3'	219bp
	Reverse	5'-ACTTGGGCTCAAACATACCG-3'	
<i>Gstm7</i>	Forward	5'-CCAAGTGTGAGGCCAAGT-3'	173bp
	Reverse	5'-CCACCTGTCAAGGTCTCTAA-3'	
<i>GAPDH</i>	Forward	5'-AACTTGGCATTGTGAAGG-3'	223bp
	Reverse	5'-ACACATGGGGGTAGGAACA-3'	

Next, the hybridized chips were washed at 60°C for 10 min in solutions of 2×SSC with 0.2% SDS, 0.1×SSC with 0.2% SDS, and 0.1×SSC, then dried at room temperature.

3.5. Detection and Analysis

The chips were scanned with a ScanArray 4000 (GSI Lumonics, Bellerica, MA) at two wavelengths, 635nm and 532 nm, to detect emission from both Cy5 and Cy3 respectively. The acquired images were analyzed using GenePix Pro 3.0 software. The intensities of each spot at the two wavelengths represent the quantity of Cy3-dUTP and Cy5-dUTP. Ratios of Cy5 to Cy3 were computed using the GenePix Pro 3.0 median of ratio method. Overall intensities were normalized using the corresponding GenePix default normalization factor. All spots flagged "Bad" or "Not Found" by GenePix software were removed from the final data. Only genes with more than 200 counts raw intensity values for both Cy3 and Cy5 were chosen for differential analysis. Genes were identified as differentially expressed if the ratio was >2 or <0.5, or the absolute value of base 2 logarithm of the ratio was >1.

3.6. Quantitative Polymerase Chain Reaction

Real-time PCR was performed using the BIO-RAD MiniOpticon Real-Time PCR System in a two-step RT-PCR. All RNA samples were treated with DNase I (Takara, Dalian, CN) to remove genomic DNA contamination. cDNA was synthesized with M-MLV reverse transcriptase (Promega, WI) according to manual instruction. Mouse specific sequences for PCR primers were designed to generate amplicons of 150 to 250 base pairs required for Real-time PCR detection using iQ SYBR Green Supermix (BIO-RAD). The mRNA abundances were determined by normalization of the data to the expression levels of glyceraldehydes -3-phosphate dehydrogenase (GAPDH) mRNA. The primers used for PCR were in table 1.

4. RESULTS AND DISCUSSIONS

4.1. LEPCs gave rise to functional hepatocyte after sodium butyrate exposure

Exposure the cultured LEPCs 2 (LEPCs clone 2) to 5 mM SB, cell growth was significantly arrested. Double nuclear cells, character of hepatocyte in vivo, can be

observed after four days in the culture (Figure 1A~1D). Ultrastructural observations provided more convincing evidence that the hepatic phenotype was induced. Before the SB treatment, the cells contained few organelles except some mitochondria and ribosome (Figure 1B). Seven days after exposure to SB, the cells contained well-developed organelles such as mitochondria, Golgi apparatus, and endoplasmic reticulum (Figure 1D). Notably, the bile canaliculus, the specific structures of mature hepatocytes, also can be observed in the intercellular space of adjacent cells (Figure 1D). The differentiation of LEPCs 2, 4, 8 and 10 (LEPCs clone 2, 4, 8 and 10) was also analyzed by RT-PCR, SB increased hepatocyte genes such as albumin, tryptophan 2,3-dioxygenase (TDO) and alcohol dehydrogenase (ADH) expression whereas decreased the expression of bile duct specific marker CK19 (Figure 1E). All the results indicated LEPCs gave rise to functional hepatocyte after SB exposure. Figure 1. LEPCs gave rise to functional hepatocyte after SB exposure.

4.2 Gene clustering of microarray data

At the transcriptome level, LEPCs, treated with SB at a series of time points, were profiled by using murine cDNA microarrays. Using GenePix Pro 3.0 software data filtering described as above, we found 796 genes represented on the cDNA microarrays to be specifically regulated differently in at least two time points in LEPCs over SB-induced differentiation. For data mining, we used SOM with the help of Genesis software, which exerts distinct advantages in both gene clustering and its visualization (15). As shown in Figure 2, the SOM outputs of the 796 genes were visualized by polygram display, offering a global view of gene clustering, particularly with respect to the expression patterns of clustered genes. Figure 2. 796 genes are clustered into 48 clusters using SOM

4.3. Sodium butyrate-mediated growth inhibition is associated with the decreased expression of cyclin B1 and Cdk4

Archer SY et al reported cyclin B1 repression was linked to the growth arrest and differentiation process in colon cancer cell HT-29 after exposure to SB (16). Agreed with previous data, accompanied with LEPCs growth arrest and differentiation, the marked decrease of

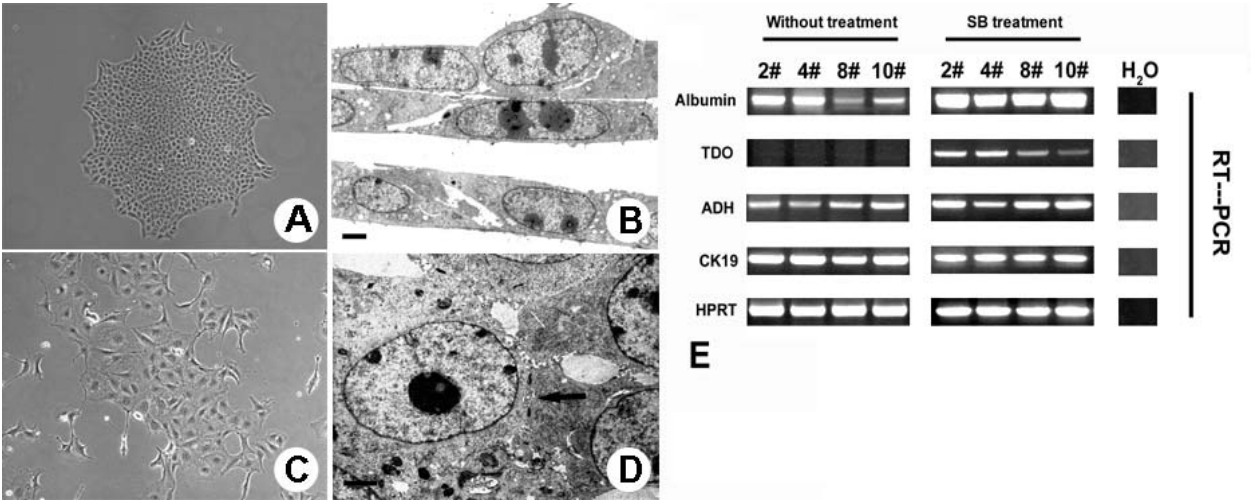


Figure 1. LEPCs gives rise to functional hepatocyte after SB exposure. The morphological varieties of LEPCs 2 after SB exposure (A~D). The phase contrast photograph (A) and electron micrograph (B) of LEPCs #2, the cells contained few organelles except some mitochondria and ribosome with high nuclear-to-cytoplasm ratio. After seven days SB exposure, double nuclear cells appeared (C). Electron micrograph showed abundant organelles and bile canaliculus structure, indicated by arrow (D). Magnification: A (100×), C (200×). Bar, 2μm. By RT-PCR analysis, the expression of hepatocyte and bile duct markers was examined on the LEPCs 2, 4, 8 and 10 after SB treatment. The PCR cycles were optimized to get the best contrast: ALB (35 cycles), TDO (40 cycles), ADH (35 cycles), CK19 (28 cycles), HPRT (30 cycles).

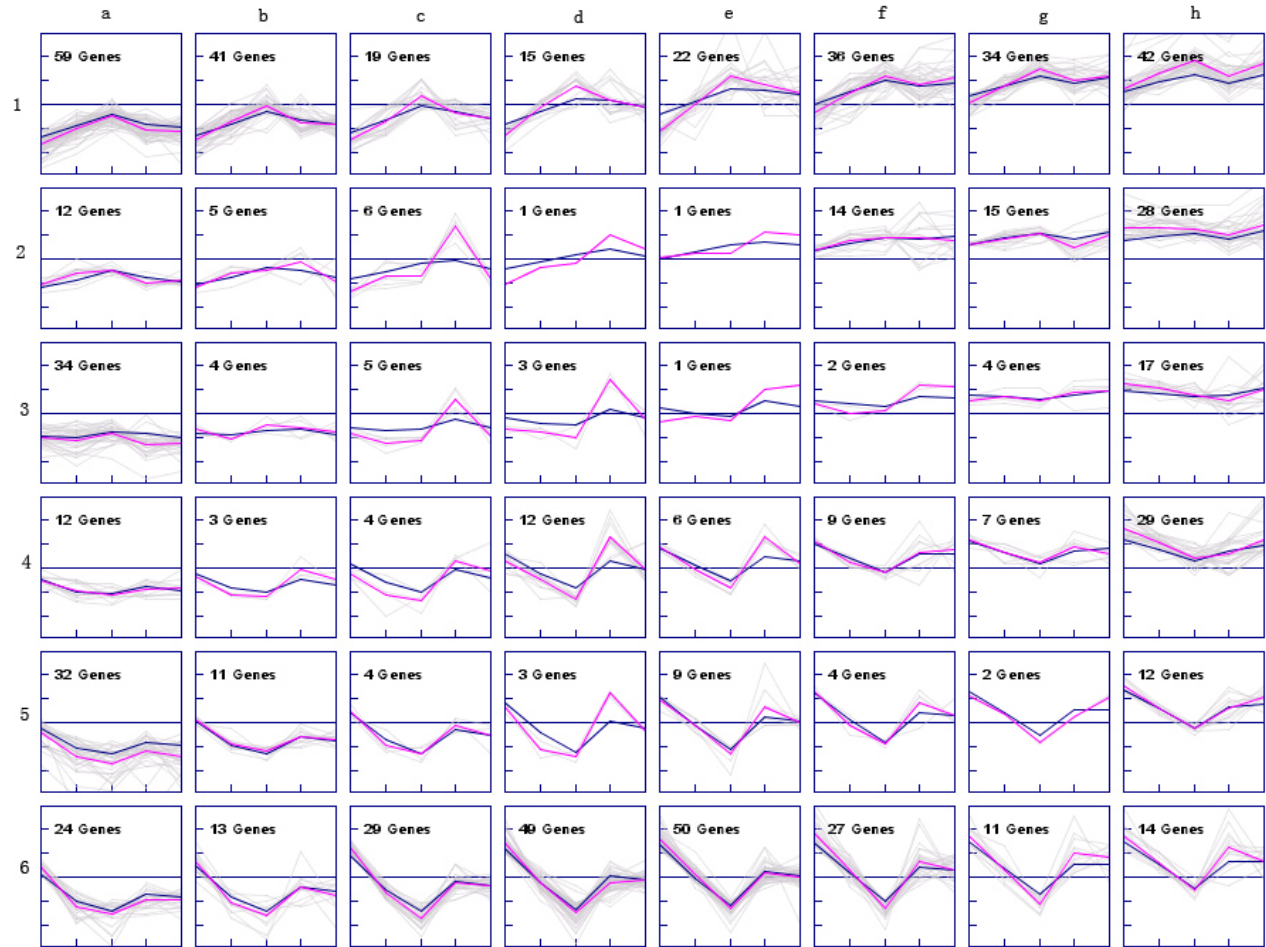


Figure 2. 796 genes are clustered into 48 clusters using SOM.

cyclin B1 and Cdk4 in mRNA levels was induced after SB treatment, meanwhile the expression of cyclin A, cyclin D and cyclin E was not altered significantly.

Notably, p21-activated kinase 1 (Pak1) was up-regulated shortly after SB treatment and remained in high level during the induction process. Recently, Leisner TM et al reported the CIB1 (calcium and integrin-binding protein 1) can inhibit tumor cell migration by binding and activating Pak1 (17). Histone deacetylase inhibitors, such as SB, have emerged as a promising class of anti-neoplastic agents by inducing tumor cell apoptosis and inhibiting metastasis (18). Our findings may highlight the key molecular mechanisms by which histone deacetylase inhibitors mediate their beneficial effects on cancer cells.

4.4. Up-regulated clusters contained mature hepatocyte functional genes which are consistent with the phenotype changes of LEPCs after SB treatment

Genes in the F-1, G-1, G-3, H-1, H-2, H-3 and H-4 clusters all are up-regulated after administration of SB, and remain in high level during the detecting period. Among these genes, many have been recognized as functional molecules of adult hepatocytes, such as tryptophan 2,3-dioxygenase (TDO), flavin containing monooxygenase 3, hydroxyacyl glutathione hydrolase, Glutathione S-transferase mu1 (GSTm1), glutathione S-transferase mu3 (GSTm3), glutathione S-transferase mu4 (GSTm4), glutamate-cysteine ligase catalytic subunit (Gclc), aldehyde dehydrogenase family 1 subfamily A1 and subfamily A7 et al, all of which are up-regulated over the induction of SB. These findings coincide with hepatic specification mentioned above.

4.5. Down-regulated clusters contained a set of genes may synergistically involved in the stemness maintaining and the process of hepatic differentiation

The clusters, containing down-regulated genes immediately after the induction, are also intensively analyzed. Especially, the genes in the a-1 cluster (listed as table 2), which are down-regulated immediately after the administration of SB and mostly remained in the low expression level during the induction, we find out that most of them are associated with transcriptional activities. Because of the relatively high expression level before differentiation, these genes may play a key role in maintaining the "stemness" of the LEPCs, and their down-regulation may ascribe to the process of hepatic differentiation.

Polycomb group (PcG) proteins form chromatin-associated, transcriptionally repressive complexes, which are critically involved in the control of cell proliferation and differentiation. Bmi1, which belongs to Polycom group proteins, acts as a negative regulator of the INK4a/ARF locus, which encodes the two tumor suppressors p16 INK4a and p19ARF (19). Bmi1 was essential to promote the proliferation of hematopoietic stem cells and inhibit apoptosis by targeting p16INK4a and p19ARF (20). Bmi1 expression by LEPCs was down-regulated abruptly after SB induction, and remain at low level throughout the time

course, which arise the possibility that Bmi1 take a significant role in the stemness maintaining and self-renewing of liver progenitors. Recent findings shown that the levels of p16INK4a are decreased in human and murine fibroblasts upon exposure to relatively high concentrations of histone deacetylase inhibitors such as trichostatin A or SB. Interestingly, the level of p19ARF is strongly up-regulated in murine cells even at low concentrations of SB (21). During LEPCs differentiation induced by SB, the interaction between Bmi1 and INK4a/ARF locus remains to be characterized.

Cellular nucleic acid-binding protein (CNBP) is a zinc finger protein that binds DNA or RNA in a sequence specific manner (22; 23). The gene of CNBP was highly conserved at the amino acid and nucleotide levels during evolution (24-30). It was shown to promote the expression of the human MYC proto-oncogene through regulating the CCCTCCCCA element (termed the CT element), which is situated 125 base pairs upstream of P1 (one of two major start sites) and consists of five imperfect direct repeats of CT element (31). During mouse embryogenesis, CNBP plays important roles in cell proliferation and tissue patterning during anterior-posterior axis, craniofacial and limb development by targeting c-Myc (32), and is essential for the forebrain induction and specification (33). Previous data also indicated c-Myc play a significant role in liver carcinogenesis. Upon Myc inactivation, liver tumors undergo proliferative arrest and cellular differentiation (34). Because of highly conservation of CNBP and its relevancy with c-Myc, the down-regulation of CNBP may promote the differentiation of LEPCs after SB exposure.

Fbxw7, which was up-regulated after SB treatment, does not clustered in a-1 cluster, but its correlation coefficients with Bmi1 and CNBP are approximate to -1 (its correlation coefficients with Bmi1 and CNBP are -0.8716 and -0.9482 respectively, calculated with Matlab software), is an F-box protein that facilitates the ubiquitination of Cyclin E, intracellular Notch1 and C-Myc (35-38). The absence of Fbxw7 results in elevated levels of cyclin E and Notch proteins (39). Cyclin E is a major regulator of the G1/S transition in mammalian cells by interaction with cyclin-dependent kinase 2. C-Myc over-expression was one of the key molecular events during liver carcinogenesis and c-Myc inactivation can induce hepatocellular cancer cells differentiat into hepatocytes and biliary cells forming bile duct structures (34). The expression of Cyclin E and C-Myc by LEPCs was not altered significantly after exposure to SB by Real-time PCR analysis (Data not show). However, because of Fbxw7 mainly regulating the target genes expression in protein levels by facilitating target proteins ubiquitination and degradation, increasing the expression of Fbxw7 would accelerate the target proteins turnover such as Cyclin E and C-Myc and therefore be associated with LEPCs cell cycle arrest and differentiation.

4.6. The authenticity of microarray data was confirmed by Real-time PCR analysis

To confirm the reliability of the data, seven selected genes were analyzed by Real-time RT-PCR, and the results were highly correlated with those of the array

Transcriptional profiling of mouse liver epithelial progenitor cells during hepatic differentiation

Table 2. Description of genes in the a-1 cluster

GenBank No.	Symbol	Gene function
AK083936	<i>Ywhah</i>	monooxygenase activity; protein domain specific binding
AB021665	<i>Trpv2</i>	DNA binding; calcium channel activity; regulation of transcription
U39073	<i>Tpmo</i>	hormone activity; protein binding; regulation of transcription
BF539304	<i>Tmem4</i>	Biological process unknown; molecular function unknown
AK090079	<i>Timm8a</i>	intracellular protein transport; protein translocase activity
AA755421	<i>Timm13a</i>	intracellular protein transport; protein translocase activity
AK083398	<i>Syncrin</i>	poly(A) binding
BU848471	<i>Sui1-rs1</i>	regulation of protein biosynthesis; translation initiation factor activity
AK084612	<i>Spc18</i>	hydrolase activity; peptidase activity; proteolysis and peptidolysis; signal peptide processing
AK090202	<i>Smfn</i>	3'-5'-exonuclease activity; hydrolase activity; manganese ion binding
AK028976	<i>Slc39a6</i>	metal ion transport; neurogenesis
AK045884	<i>Sfrs7</i>	RNA binding; nuclear mRNA splicing, via spliceosome
NM_026499	<i>Sfrs6</i>	RNA binding; nuclear mRNA splicing, via spliceosome
AK081302	<i>Sfrs3</i>	RNA binding; mRNA splice site selection; spliceosome complex
BC033603	<i>Sfpq</i>	biological process unknown; cellular component unknown; nucleic acid binding
AK036616	<i>Rnu22</i>	protein binding
NM_133832	<i>Rdh10</i>	oxidoreductase activity
AK011224	<i>Rbm3</i>	RNA binding; nucleic acid binding
NM_011184	<i>Psm3</i>	endopeptidase activity; proteasome core complex (sensu Eukarya); ubiquitin-dependent protein catabolism
AK010300	<i>Pole4</i>	DNA binding; DNA-directed DNA polymerase activity
NM_008880	<i>Plscr2</i>	calcium ion binding; integral to membrane
AK003628	<i>Plscr1</i>	calcium ion binding; integral to membrane
AK032172	<i>Pabpn1</i>	mRNA polyadenylation; nucleic acid binding; poly(A) binding
BC057002	<i>Osp94</i>	ATP binding; chaperone activity; heat shock protein activity
BC005784	<i>Nup62</i>	nucleocytoplasmic transport; nucleocytoplasmic transporter activity
BQ044164	<i>null</i>	molecular function unknown
BQ043986	<i>Nme-M1</i>	nucleoside-diphosphate kinase activity; transferase activity
BE987481	<i>MGC36453</i>	molecular function unknown
BC018353	<i>Hnrpu</i>	ribonucleoprotein complex; viral nucleocapsid
BC016459	<i>Hnrph1</i>	nucleic acid binding; ribonucleoprotein complex
BG173448	<i>H2afz</i>	DNA binding; chromosome organization and biogenesis (sensu Eukarya); nucleosome assembly
AK083453	<i>Gas5</i>	molecular function unknown
BC052366	<i>Fez2</i>	protein binding
AK033002	<i>Fbl</i>	Cajal body; RNA binding; rRNA processing; ribonucleoprotein complex; snoRNA binding
BI735498	<i>Eef1e1</i>	protein biosynthesis; translation elongation factor activity
NM_017397	<i>Ddx20</i>	ATP-dependent helicase activity; negative regulation of transcription from Pol II promoter; transcriptional repressor activity
NM_025860	<i>Ddx18</i>	ATP binding; helicase activity; hydrolase activity
BC058723	<i>Cnbp</i>	cholesterol biosynthesis; positive regulation of transcription from Pol II promoter
AK047055	<i>Cdc26</i>	peptidyl-prolyl cis-trans isomerase activity
XM_131189	<i>C330027G06Rik</i>	molecular function unknown
M64279	<i>Bmi1</i>	cell growth and/or maintenance; chromatin modification; regulation of transcription
AK129071	<i>Bclaf1</i>	negative regulation of transcription; positive regulation of apoptosis
BQ936229	<i>Banf1</i>	DNA binding; DNA integration; provirus integration
M11310	<i>Aprt</i>	adenine phosphoribosyltransferase activity
AK076467	<i>Anxa3</i>	calcium-dependent phospholipid binding; phospholipase A2 inhibitor activity
AK017504	<i>5730406I15Rik</i>	endoplasmic reticulum; hydrolase activity; integral to membrane; peptidase activity
BC029173	<i>Mrpl47</i>	structural constituent of ribosome
AK012674	<i>2810004N20Rik</i>	hydrolase activity
AK077261	<i>2700089E24Rik</i>	molecular function unknown
BC031521	<i>2700023B17Rik</i>	molecular function unknown
BM899018	<i>2610012O22Rik</i>	molecular function unknown
BC025430	<i>Trim59</i>	molecular function unknown
AK029037	<i>1700034H14Rik</i>	molecular function unknown
BC048184	<i>Wwp2</i>	ligase activity; protein modification; ubiquitin cycle; ubiquitin-protein ligase activity
AK003739	<i>1110017C15Rik</i>	RNA binding
AK078599	<i>0610009I22Rik</i>	integral to membrane; phospholipid biosynthesis; transferase activity
BC069915	<i>Pcbp1</i>	translation activator activity
BF164657	<i>Rps3a</i>	structural constituent of ribosome
BU700474	<i>null</i>	molecular function unknown
CN842571	<i>null</i>	molecular function unknown

data. Because these selected genes either down-regulated or up-regulated through out all timepoints after induction of SB, we compare the average expression of all the timepoints between the two different methods. Representative results of seven genes are shown in Figure 3. Figure 3. The authenticity of microarray data was confirmed by analyzing the expression of selected genes by quantitative Real-time PCR.

Briefly, in this report, we described the hepatic specification of cultured liver epithelial progenitor cells (LEPCs) upon exposure to sodium butyrate. Gene expression profile during the hepatic differentiation of LEPCs was analyzed by murine cDNA microarray. Consistent with the phenotype change of LEPCs after sodium butyrate treatment, many hepatocyte functional

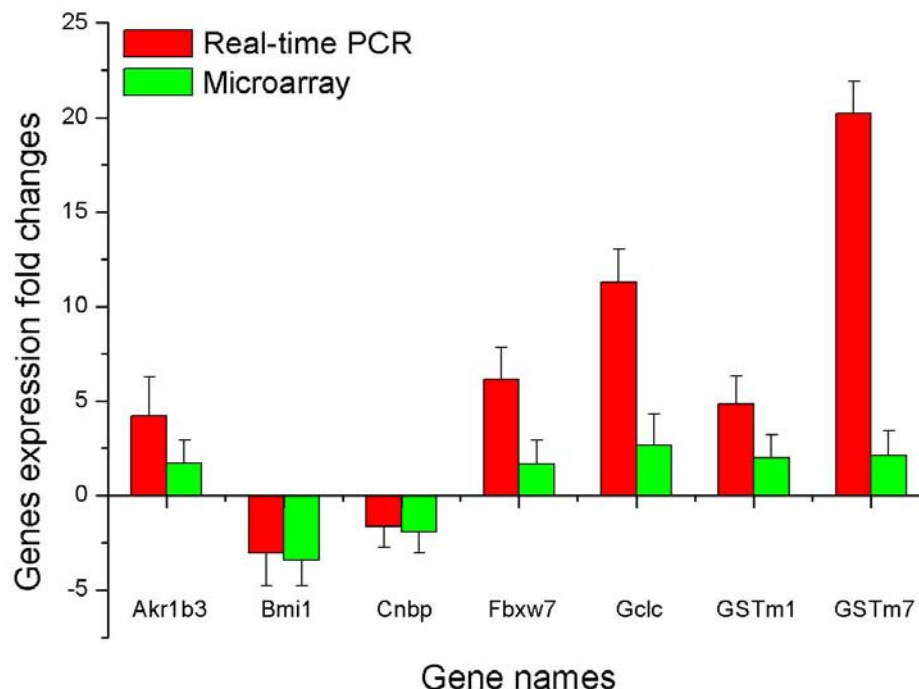


Figure 3. The authenticity of microarray data confirmed by quantitative Real-time PCR.

genes are up-regulated. Moreover, some molecular clues, mediating LEPCs growth, stemness and differentiation, were also revealed. In conclusion, our data reflected a global view of the expression pattern during the hepatic differentiation of LEPCs induced by sodium butyrate.

5. ACKNOWLEDGEMENT

This research was supported by a grant 2002AA2Z2002 from the National High Technology Research and Development Program of China (863 Program) and National Nature Science Foundation (No. 30270668, 30200138). Dr Wenlin Li, and Pu You contributed equally to this study.

6. REFERENCES

1. Theise N.D.: Gastrointestinal stem cells. III. Emergent themes of liver stem cell biology: niche, quiescence, self-renewal, and plasticity. *Am J Physiol Gastrointest Liver Physiol* 290, G189-193 (2006)
2. Sarraf C., E. Lalani, M. Golding, T.V. Anilkumar, R. Poulosom, M. Alison: Oval cell activation in the rat liver. *Am J Pathol* 145, 1114-1126 (1994)
3. Van Eyken P., R. De Vos, V.J. Desmet: Progenitor ("stem") cells in alcoholic liver disease? In Hall P, editor. *Alcoholic liver disease: Pathology and pathogenesis*. 2nd ed. London: Edward Arnold: 160-171 (1995)
4. Lenzi R., M.H. Liu, P.A. Slott: Histogenesis of bile duct-like cells proliferating during ethionine hepatocarcinogenesis. Evidence for a biliary epithelial nature of oval cells. *Lab Invest* 66, 390-402 (1992)
5. Lemire J.M., N. Shiojiri, N. Fausto: Oval cell proliferation and the origin of small hepatocytes in liver

- injury induced by D-galactosamine. *Am J Pathol* 139, 535-552 (1991)
6. Sell S.: Heterogeneity and plasticity of hepatocyte lineage cells. *Hepatology* 33, 738-750 (2001)
7. Plescia C., C. Rogler, L. Rogler: Genomic expression analysis implicates Wnt signaling pathway and extracellular matrix alterations in hepatic specification and differentiation of murine hepatic stem cells. *Differentiation* 68, 254-269 (2001)
8. Suzuki A., A. Iwama, H. Miyashita, H. Nakauchi, H. Taniguchi: Role for growth factors and extracellular matrix in controlling differentiation of prospectively isolated hepatic stem cells. *Development* 130, 2513-2524 (2003)
9. Pack R., R. Heck, H.P. Dienes: Isolation, biochemical characterization, long-term culture, and phenotypic modulation of oval cells from carcinogen-fed rats. *Exp Cell Res* 204, 198-209 (1993)
10. Schena M., D. Shalon, R.W. Davis, P.O. Brown: Quantitative monitoring of gene expression patterns with a complementary DNA microarray. *Science* 270, 467-470 (1995)
11. Schena M, D. Shalon, R. Heller, A. Chai, P.O. Brown, R.W. Davis: Parallel human genome analysis: microarraybased expression monitoring of 1000 genes. *PROC NATL ACAD SCI USA* 93, 10614-10619 (1996)
12. Li W.L., J. Su, Y.C. Yao, X.R. Tao, Y.B. Yan, H.Y. Yu, X.M. Wang, J.X. Li, Y.J. Yang, J.T.Y. Lau, Y.P. Hu: Isolation and Characterization of Bipotent Liver Progenitor Cells from Adult Mouse. *Stem Cells* 24, 322-332 (2006)
13. Brown P.: In: <http://cmgm.stanford.edu/pbrown/protocols/index.html>[0] (2000)
14. Sambrook J., D.W. Russell: Using PCR to amplify DNA *in vitro*. In: *Molecular Cloning: A Laboratory*

Manual, 3rd ed. Eds: *Cold Spring Harbor Laboratory Press*, NY (2001)

15. Xiao L., K. Wang, Y. Teng, J. Zhang: Component plane presentation integrated self-organizing map for microarray data analysis. *FEBS Lett* 538, 117-124 (2003)

16. Archer SY, Johnson J, Kim HJ, Ma Q, Mou H, Daesety V, Meng S, Hodin RA: The histone deacetylase inhibitor butyrate down-regulates cyclin B1 gene expression via a p21/WAF-1-dependent mechanism in human colon cancer cells. *Am J Physiol Gastrointest Liver Physiol* 289, G696-703 (2005)

17. Leisner T.M., M. Liu, Z.M. Jaffer, J. Chernoff, L.V. Parise: Essential role of CIB1 in regulating PAK1 activation and cell migration. *J Cell Biol* 170, 465-476 (2005)

18. Johnstone R.W., J.D. Licht: Histone deacetylase inhibitors in cancer therapy: is transcription the primary target? *Cancer cell* 4, 13-18 (2003)

19. Jacobs J.J., K. Kieboom, S. Marino, R.A. DePinho, M. van Lohuizen: The oncogene and Polycomb-group gene Bmi1 regulates cell proliferation and senescence through the ink4a locus. *Nature* 397, 164-168 (1999)

20. In-kyung P., D.L. Qian, M. Kiel, M.W. Becker, M. Pihlaja, I.L. Weissman, S.J. Morrison, M.F. Clarke: Bmi1 is required for maintenance of adult self-renewing haematopoietic stem cells. *Nature* 423, 302-305 (2003)

21. Matheu A., P. Klatt, M. Serrano: Regulation of the INK4a/ARF Locus by Histone Deacetylase Inhibitors. *J Biol Chem* 280, 42433-42441 (2005)

22. Klug A., D. Rhodes: Zinc fingers: a novel protein motif for nucleic acid recognition. *Cold Spring Harb Symp Quant Biol* 52, 473-482 (1987)

23. Saotome Y., C.G. Winter, D. Hirsh: A widely expressed novel C2H2 zinc-finger protein with multiple consensus phosphorylation sites conserved in mouse and man. *Gene* 152, 223-233 (1995)

24. Rajavashisth T.B., A.K. Taylor, A. Andalibi, K.L. Svenson, A.J. Lusis: Identification of a zinc finger protein that binds to the sterol regulatory element. *Science* 245, 640-643 (1989)

25. Warden C.H., S.K. Krisans, D. Purcell-Huynh, L.M. Leete, A. Daluiski, A. Diep, B.A. Taylor, A.J. Lusis: Mouse cellular nucleic acid binding proteins: a highly conserved family identified by genetic mapping and sequencing. *Genomics* 24, 14-19 (1994)

26. Yasuda J., S. Mashiyama, R. Makino, S. Ohyama, T. Sekiya, K. Hayashi: Cloning and characterization of rat cellular nucleic acid binding protein (CNBP) cDNA. *DNA Res* 2, 45-49 (1995)

27. Van Heumen W.R., C. Claxton, J.O. Pickles: Sequence and tissue distribution of chicken cellular nucleic acid binding protein cDNA. *Comp Biochem Physiol B Biochem Mol Biol* 118, 659-665 (1997)

28. Flink I.L., I. Blitz, E. Morkin: Characterization of cellular nucleic acid binding protein from *Xenopus laevis*: expression in all three germ layers during early development. *Dev Dyn* 211, 123-130 (1998)

29. Armas P., M.O. Cabada, N.B. Calcaterra: Primary structure and developmental expression of *Bufo arenarum* cellular nucleic acid binding protein: changes in subcellular localization during early embryogenesis. *Dev Growth Differ* 43, 13-23 (2001)

30. Armas P, S. Cachero, V.A. Lombardo, A. Weiner, M.L. Allende, N.B. Calcaterra: Zebrafish cellular nucleic acid-binding protein: gene structure and developmental behaviour. *Gene* 337, 151-161 (2004)

31. Michelotti E.F., T. Tomonaga, H. Krutzsch, D. Levens: Cellular nucleic acid binding protein regulates the CT element of the human c-Myc protooncogene. *J Biol Chem* 270, 9494-9499 (1995)

32. Shimizu K, W. Chen, A.M. Ashique, R. Moroi, Y.P. Li: Molecular cloning, developmental expression, promoter analysis and functional characterization of the mouse CNBP gene. *Gene* 307, 51-62 (2003)

33. Chen W., Y. Liang, W. Deng, K. Shimizu, A.M. Ashique, E. Li, Y.P. Li: The zinc-finger protein CNBP is required for forebrain formation in the mouse. *Development* 130, 1367-1379 (2003)

34. Shachaf C.M., A.M. Kopelman, C. Arvanitis, A. Karlsson, S. Beer, S. Mandl, M.H. Bachmann, A.D. Borowsky, B. Ruebner, R.D. Cardiff, Q.W. Yang, J.M. Bishop, C.H. Contag, D.W. Felsher: MYC inactivation uncovers pluripotent differentiation and tumour dormancy in hepatocellular cancer. *Nature* 431, 1112-1117 (2004)

35. Gupta-Rossi N., O. Le Bail, H. Gonen, C. Brou, F. Logeat, E. Six, A. Ciechanover, A. Israel: Functional interaction between SEL-10, an F-box protein, and the nuclear form of activated Notch1 receptor. *J Biol Chem* 276, 34371-34378 (2001)

36. Moberg K.H., D.W. Bell, D.C. Wahrer, D.A. Haber, I.K. Hariharan: Archipelago regulates Cyclin E levels in *Drosophila* and is mutated in human cancer cell lines. *Nature* 413, 311-316 (2001)

37. Koepp D.M., L.K. Schaefer, X. Ye, K. Keyomarsi, C. Chu, J.W. Harper, S.J. Elledge: Phosphorylation-dependent ubiquitination of cyclin E by the SCFFbxw7 ubiquitin ligase. *Science* 294, 173-177 (2001)

38. Yada M., S. Hatakeyama, T. Kamura, M. Nishiyama, R. Tsunematsu, H. Imaki, N. Ishida, F. Okumura, K. Nakayama, K.I. Nakayama: Phosphorylation-dependent degradation of c-Myc is mediated by the F-box protein Fbxw7. *EMBO* 23, 1112-1117 (2004)

39. Tetzlaff M.T., W. Yu, M. Li, P. Zhang, M. Finegold, K. Mahon, J.W. Harper, R.J. Schwartz, S.J. Elledge: Defective cardiovascular development and elevated cyclin E and Notch proteins in mice lacking the Fbxw7 F-box protein. *Proc Natl Acad Sci U S A* 101, 3338-3345 (2004)

Key Words: Hepatic Stem Cells, Liver, Hepatocyte, Differentiation, Sodium Butyrate

Send correspondence to: Yiping Hu, Department of Cell Biology, Second Military Medical University, Xiangyin Road 800, Shanghai 200433, P. R. China, Phone: 8621-25070291, Fax: 8621-25070293, E-mail: yphu@suum.edu.cn.

<http://www.bioscience.org/current/vol12.htm>